The Dynamics of Quantum Computing in Molecules

9

Alex Brown and Ryan R. Zaari

Abstract

A brief introduction to quantum computing is provided and the potential use of molecules as the platform is discussed. The basic building blocks (quantum bits, quantum gates, and quantum algorithms) are described in order to emphasize the requirements for realizing a quantum computer, and, the advantages quantum computation has over its classical counterpart. We outline the three key steps to quantum computation: (1) initialization, (2) manipulation, and (3) readout. The possible use of internal molecular states as quantum bits and shaped laser fields to implement the quantum gates is introduced. The application to molecular quantum computing is connected to the more general problem of the control of quantum dynamics using tailored laser fields determined theoretically with optimal control theory or genetic algorithms.

9.1 The Advent of Quantum Computing

The rapid pace of computer technology innovation was predicted in the early 1960s by Intel co-founder Gordon Moore. His prediction, popularly known as "Moore's Law," states that transistor density on integrated circuits (a rough measure of computer processing power) doubles about every 2 years. While this "Law" has held for nearly 50 years, the end is in sight. However, more than 30 years

A. Brown (✉)
Department of Chemistry, University of Alberta, Edmonton, AB, Canada T6G 2G2
e-mail: alex.brown@ualberta.ca

R.R. Zaari
Department of Chemistry, University of Alberta, Edmonton, AB, Canada T6G 2G2

Present Address: Department of Chemistry, University of Nevada, 216, Reno, NV 89557-0216, USA
e-mail: rzaari@ualberta.ca

F. Gatti (ed.), *Molecular Quantum Dynamics*, Physical Chemistry in Action,
DOI 10.1007/978-3-642-45290-1_9,

ago, the physicist Richard Feynman proposed a potentially revolutionary idea for computation: the quantum computer [1]. By utilizing quantum mechanical phenomena, such as quantum superposition, entanglement, and interference, a quantum computer realizes a fundamentally new mode of information processing relative to classical computing [2, 3]. The quantum computing paradigm opens the avenue to vast increases in computational power relative to methods based on classical computation. Several potential applications of quantum computing are already known: cryptography, algorithmic searching, and factorizing large numbers very rapidly. Of particular interest to the field of molecular simulation, the advent of quantum computing would allow the efficient simulation of quantum-mechanical systems over unprecedented length and time scales. With the potential benefits being so great, the field of quantum computing has emerged as an intriguing and exciting research area involving the efforts of chemists, computer scientists, engineers, mathematicians, and physicists.

In the present work, a brief introduction to the basic ideas of quantum computing is provided. In particular, several problems that need to be addressed in order to realize a quantum computer are introduced: the identification of a physical system to represent the quantum bits (qubits), the implementation of mechanisms for performing quantum logic gate operations on the qubits, and the maintenance of coherence. While several different physical systems have been proposed or utilized to realize quantum computing algorithms[4–8], the focus here is on the use of molecules to store the quantum information and shaped laser pulses to carry out the quantum gate operation—ideas introduced over 10 years ago [9–11]. Here the proposals for implementing qubits in molecular systems are introduced, and the methodologies for finding the shaped laser pulses (i.e., optimal control theory (OCT) and genetic algorithms [12–14]) are discussed. Since a theoretical understanding of these problems requires solving the time-dependent Schrödinger equation (TDSE), there is a strong connection to the field of quantum dynamics and new ideas and methods developed in that area can have important applications in the field of molecular quantum computing.

9.1.1 Qubits, Quantum Gates and Quantum Algorithms

The computers that we encounter in our everyday lives operate using *classical* processing. On the most fundamental level, calculations occur by changes in the state of bits which can be in either of two states; typically represented by a “0” or “1” in binary notation. The changes in the state of bits occurs by boolean logic operations such that a specific sequence of these logic operations can carry out an algorithm. It is these algorithms that are used to perform computations. The workings of a quantum computer are (to-date) analogous to a classical computer. However, the quantum mechanical nature of a system and its interactions are utilized to represent qubits, quantum logic gate operations and quantum algorithms. As stated before, a classical bit can exist in one of the two states (0 or 1) but a qubit is a quantum 2-state system; although qudits with d quantum states could be

used, we restrict our discussion to qubits only. The resulting state of the qubit is a superposition of both "0" and "1". For example, a classical two-bit system can be in one of the four possible states, i.e., "00", "01", "10" or "11" state. A quantum two-qubit system, represented in Dirac notation as $|q_1 q_2\rangle$, can be in pure states $|00\rangle$, $|01\rangle$, $|10\rangle$ and $|11\rangle$. The critical difference to classical bits is that qubits are described by the wavefunction, $\Psi = \sum_{q_1,q_2=0}^{1} c_{q_1,q_2}|q_1 q_2\rangle$, where the coefficients c_{q_1,q_2} have the relationship $\sum_{q_1,q_2} |c_{q_1,q_2}|^2 = 1$. Therefore, the system (i.e., the quantum information) is represented by the superposition of its individual qubits—it is this fundamental difference that leads to the power of quantum computing (see Sect. 9.1.3). With respect to the representation, qubits can be structured in two different ways. The first case entails that each qubit is represented by a separate 2-level or quasi 2-level system, and then these n qubits are appropriately coupled [6,15–17]. This is the case, for example, in ion trap quantum computing examples in which a string of trapped atomic ions represents a series of qubits through excitation of two hyperfine levels from each atom, while coupling between each atom/qubit occurs through vibrational motion in the harmonic potential of the linear Paul trap [4, 17]. Alternatively, n qubits can be represented by $N = 2^n$ combinations of N quantum states [18–20]. A proposed quantum computing architecture suggests using the rovibrational states or modes of molecules as qubits and in this case each resulting qubit state,"00" to "11", would be represented as the qubits. In this case n qubits are represented by 2^n quantum states [9]. Quantum logic gates have specific requirements due to their quantum mechanical nature. Unlike classical logic gates, a quantum logic gate ($\mathbf{Q}$) must be reversible ($\mathbf{Q}\mathbf{Q}^{-1} = \mathbb{1}$), unitary ($\mathbf{Q}^\dagger = \mathbf{Q}^{-1}$) and Hermitian ($\mathbf{Q}^\dagger = \mathbf{Q}$)—if these requirements were not fulfilled, it would indicate decoherence in the system leading to the loss of quantum information. There are a number of elementary quantum logic gates such as the NOT, Controlled-NOT (CNOT), Hadamard, Toffoli and phase gates as shown in Table 9.1, which can be used for universal quantum computation (see Sect. 9.1.5). In order to illustrate the general operation of a quantum gate, consider a NOT gate acting on the general quantum state, $\Psi = c_0|0\rangle + c_1|1\rangle$, i.e.,

$$\text{NOT}\Psi = \begin{pmatrix} 0 & 1 \\ 1 & 0 \end{pmatrix} \begin{pmatrix} c_0 \\ c_1 \end{pmatrix} = \begin{pmatrix} c_1 \\ c_0 \end{pmatrix} = c_1|0\rangle + c_0|1\rangle. \tag{9.1}$$

The extension to 2-qubit and n-qubit gate operations is straightfoward.

An example algorithm is the one-bit full adder which is shown in Table 9.2 for the classical and quantum forms of the algorithm [21]. The one-bit adder adds three one-bit numbers (A, B and C_{in}) to produce output bits ($S = A + B + C_{in}$ and C_{out}). The carry (C_{in} and C_{out}) are bits from previous or future additions, respectively, as would occur if the sum of the numbers, S, is greater than or equal to two. This is analogous to addition in the decimal system, as when the number is greater than or equal to 10 then we carry a 1 to the next place value. The quantum form of the one-bit adder must include one additional input (D) and two extra

Table 9.1 Examples of elementary quantum logic gates in matrix notation

Gate	Matrix operation	Gate	Matrix operation
NOT	$\begin{pmatrix} 0 & 1 \\ 1 & 0 \end{pmatrix}$	CNOT	$\begin{pmatrix} 1 & 0 & 0 & 0 \\ 0 & 1 & 0 & 0 \\ 0 & 0 & 0 & 1 \\ 0 & 0 & 1 & 0 \end{pmatrix}$
Phase	$\begin{pmatrix} 1 & 0 \\ 0 & e^{i\theta} \end{pmatrix}$		
Hadamard	$\frac{1}{\sqrt{2}} \begin{pmatrix} 1 & 1 \\ 1 & -1 \end{pmatrix}$	Toffoli	$\begin{pmatrix} 1 & 0 & 0 & 0 & 0 & 0 & 0 & 0 \\ 0 & 1 & 0 & 0 & 0 & 0 & 0 & 0 \\ 0 & 0 & 1 & 0 & 0 & 0 & 0 & 0 \\ 0 & 0 & 0 & 1 & 0 & 0 & 0 & 0 \\ 0 & 0 & 0 & 0 & 1 & 0 & 0 & 0 \\ 0 & 0 & 0 & 0 & 0 & 1 & 0 & 0 \\ 0 & 0 & 0 & 0 & 0 & 0 & 0 & 1 \\ 0 & 0 & 0 & 0 & 0 & 0 & 1 & 0 \end{pmatrix}$

In general the Hadamard, Phase and NOT gates are 1-qubit operations, the CNOT gate is a 2-qubit operation, and the Toffoli is a 3-qubit operation

Table 9.2 Description of the classical and quantum one-bit full adder algorithm

Inputs				Outputs			
C_{in}	A	B	D	C_{in}	A	S	C_{out}
0	**0**	**0**	0	0	0	**0**	**0**
1	**0**	**0**	0	1	0	**1**	**0**
0	**1**	**0**	0	0	1	**1**	**0**
1	**1**	**0**	0	1	1	**0**	**1**
0	**0**	**1**	0	0	0	**1**	**0**
1	**0**	**1**	0	1	0	**0**	**1**
0	**1**	**1**	0	0	1	**0**	**1**
1	**1**	**1**	0	1	1	**1**	**1**

The input binary numbers (C_{in}, A, B) are added to produce the output numbers (S, C_{out}). The carry (C_{in}, C_{out}) represent the bits being carried over from previous and future additions, respectively. Additional input (D) and output (A, C_{in}) binary numbers are included in the quantum form of the algorithm to ensure reversibility. The inputs and outputs for the classical one-bit adder are given in bold while the quantum algorithm requires all four inputs to produce all four outputs

output (A, C_{in}) qubits to ensure reversibility. In order to illustrate the concept of irreversibility in the classical form of the algorithm, consider the following three inputs (C_{in},A,B) = (**100**), (**010**) and (**001**), see Table 9.2. All three produce the same final state (S, C_{out}) = (**10**), and hence, one could not reversibly return from this output to the correct initial state. If the input (D) and output (A, C_{in}) qubits are included in the quantum algorithm, the input states (**100**0), (**010**0) and (**001**0) now produce different final states (10**10**), (01**10**) and (00**10**), respectively, albeit all with the same values of (S, C_{out}) = (**10**). However, since the final states are distinct, the process could be reversed to return to the corresponding initial state. The quantum

Table 9.3 An example of the general phase imposed after the NOT_2 quantum gate is applied

Gate	Matrix operation	Global phase alignment
NOT_2	$\begin{pmatrix} 0 & 1 & 0 & 0 \\ 1 & 0 & 0 & 0 \\ 0 & 0 & 0 & 1 \\ 0 & 0 & 1 & 0 \end{pmatrix}$	$\|00\rangle \rightarrow \|01\rangle e^{i\phi_1}$ $\|01\rangle \rightarrow \|00\rangle e^{i\phi_2}$ $\|10\rangle \rightarrow \|11\rangle e^{i\phi_3}$ $\|11\rangle \rightarrow \|10\rangle e^{i\phi_4}$

Each gate operation on each qubit acquires an arbitrary phase, $e^{i\phi_n}$

one-bit full adder algorithm can be implemented with the elementary Toffoli and CNOT quantum logic gates [21]. A finite number of elementary boolean logic gates provides the means to produce a vast number of algorithms. This is similar to the finite set of letters in an alphabet (logic gates) which produce a vast number of words, sentences and books in a language (algorithm).

9.1.2 Global Phase Alignment

In order to implement a quantum algorithm, a series of quantum gates must be applied in a specific order. Therefore, besides causing the required qubit excitations, there is an extra requirement imposed on the laser pulse quantum gate operation. That is, the laser pulse quantum gate operation must also align the relative phases of all the qubits by the end of the laser pulse interaction. This is termed *global phase alignment*. Thus subsequent application of quantum gates will impose the appropriate qubit transformation, since the qubits will all be in phase. An example of this is shown in Table 9.3 for the 2-qubit NOT gate or NOT_2 quantum logic gate. If a laser pulse were applied that does not impart a global alignment in qubit phase, then there would be an arbitrary resultant phase associated with each qubit. Subsequent quantum gate transformations would impart even more phase uncertainty. Global phase alignment requires that all resultant phases are the same and in the case of the example NOT_2 gate, $e^{i\phi_1} = e^{i\phi_2} = e^{i\phi_3} = e^{i\phi_4}$. The control of qubit phase is important within many quantum algorithms and some quantum logic gates.

9.1.3 Quantum Superpositions and Quantum Parallelism

It may now seem apparent that an advantage of a quantum computer is in its ability to construct superpositions of qubits, something not possible on a classical computer. During each computation the system's wavefunction consisting of superpositions of the qubits (in reality the wavefunction likely also contains some other non-qubit states) is manipulated according to the necessary quantum logic gates required by the algorithm. Thus every qubit experiences each quantum gate operation, in turn each qubit is manipulated by the entire quantum algorithm and at the end of the computation the wavefunction exists which describes every

possible solution from each initial condition. By contrast, in order to attempt representing this on a classical computer would require one processor for each qubit and then run in parallel to produce all possible solutions to all possible initial conditions. Thus *quantum parallelism* is not the same as classical parallelism since classical parallelism refers to using multiple processors and on a quantum computer this is done on the single processor. Quantum parallelism was first described by Deutsch [22].

9.1.4 Advantages of a Quantum Computer

By utilizing quantum behaviour, algorithms can be constructed on a quantum computer which in some cases take exponentially less computational time as compared to classical computers. The most recognized quantum algorithm is Shor's algorithm [23] for factoring prime numbers. It was shown that a quantum computer implementing Shor's algorithm could determine the factors of a prime number in a polynomial amount of time; the classical counterpart requires an exponential amount of time with respect to the size of the prime number. Even though it is relatively straightforward to generate very large valued prime numbers, it is exceptionally difficult to determine their resulting factors on a classical computer. It is this key classical computing limitation that allows Internet RSA encryption to function. Using Shor's algorithm, the prime factors of 15 were calculated through Nuclear Magnetic Resonance (NMR) using 7 spin 1/2 nuclei of a perfluorobutadienyl iron complex as the qubits [6]. This is the largest number of qubits used in an NMR quantum computation. The Deutsch–Jozsa algorithm, an example quantum algorithm which performs exponentially faster on a quantum computer, has also been applied as a benchmark to many quantum computer systems [17, 19].

Recent developments in quantum algorithms showcase specific uses in mathematics, physics and chemistry with much improved calculation times compared to our current classical computers. In current electronic structure calculations, the CPU time required to compute molecular energies scales exponentially with the system size but it has been shown to take only a polynomial amount of time on a quantum computer [24]. Chemical reactions could also be simulated exactly on a quantum computer in polynomial time with respect to the system size [25]. Other example studies have deduced quantum algorithms for determining the dynamics of open quantum systems [26] and also molecular properties and geometry optimizations [27]. With respect to molecular dynamics simulations, a true quantum Metropolis algorithm has been developed [28] and also a quantum algorithm for exact Monte Carlo sampling [29]. Quantum algorithms within mathematics have also been developed for systems of linear equation [30] and for solving the Poisson equation [31]. These select examples of the implementation of quantum algorithms in science and mathematics showcase the inherent and valuable use a quantum computer would have for scientific research.

9.1.5 Universal Quantum Computer and Quantum Simulator

Thus far, the largest universal quantum computer controlled 14 qubits represented by 14 $^{40}Ca^{+}$ cations (one for each qubit) in a linear Paul ion trap [32], but it has been suggested that thousands or even millions of qubits would be needed to perform a practical calculation [33, 34]. On this 14-qubit quantum computer, the authors investigated entanglement and the effect of noise, but being a universal quantum computer they could have examined other simple quantum algorithms. The most recent applicable progress has been made by utilizing a quantum algorithm on a linear optical quantum simulator for determining eigenvalues of a molecule and the hydrogen molecule was used as the simplest test case [35]. A universal quantum computer would have the capability of solving general quantum algorithms whereas a quantum simulator would solve a problem specific to the system being "simulated" [21]. Using the previously described one-bit full adder as an example, a universal quantum computer would utilize a specific set of universal quantum logic gates to represent the quantum analogue of the one-bit full adder, whereas a quantum simulator would be designed strictly to carry out the one-bit full addition operation only.

9.1.6 Experimentally Realized and Proposed Quantum Computer Architectures

Besides the inherent properties that a quantum computer, including the quantum gates, must have, there are technical issues regarding implemented and proposed architectures. These issues include scalability, decoherence and computational speed. Scalability refers to the ability to increase the number of qubits for calculation. Coherence is the ability for the qubit to retain its encoded information and thus decoherence is a loss of encoded information. Computational speed refers to the general number of quantum gates that can be applied before decoherence destroys the quantum state information. As will be alluded to below, it is not so much the difference between atoms and molecules in quantum computing architectures that determines feasibility but more so the choice of quantum state for qubit representation.

The current implementation of a quantum computing architecture utilizing atoms comes in the form of linear Paul ion traps [4], though there are suggestions of performing quantum algorithms on atomic ions that are trapped in a 2-D or 3-D lattice [5]. The qubits are represented by two hyperfine atomic levels, generally chosen to be the ground state and some metastable state. With these choices of quantum states, information encoded in the qubits can be long lived with respect to the quantum operation being performed, and qubit preparation (see Sect. 9.2.1) is straightforward through known atomic "cooling" techniques. Just as important, the system is scalable simply by adding more atomic ions to the linear Paul trap. The qubit excitations correspond to frequencies in the microwave region and qubit

coupling occurs through vibrational mode coupling in the linear Paul harmonic trap. Due to this, the application of a series of laser pulses to represent quantum logic gates combined with the slow harmonic vibrational coupling could lead to decoherence before the end of the quantum computation.

Alternatively a quantum computing architecture that has shown promise but uses molecules is that of NMR [6–8]. The qubits are represented by the nuclear spin of specific atoms within the molecule. Again the lifetimes for such states are long lived and qubit state preparation is done through familiar NMR techniques. Scalability is an issue for NMR quantum computing since increasing the number of qubits requires increasing the number of nuclei in the molecule (i.e. increasing the size of the molecule). In conjunction with scalability, the molecules used in NMR quantum computing are specifically designed such that the nuclear spin excitations occur in distinctly separate regions of the energy spectrum for detection purposes. The qubit excitations occur through application of radiofrequency pulses and the qubits are coupled through J-coupling of nuclei. Again very long radiowaves could lead to decoherence before application of the entire quantum algorithm.

In order to attempt at circumventing some of the problems encountered in current quantum computer implementations, it was proposed that rovibrational states or vibrational modes of molecules could be used to represent the qubits [9]. Qubits are coupled through strong intermolecular dipole–dipole coupling and/or intermolecular vibrational mode coupling. Respective qubit excitations occur in the mid-infrared using femtosecond laser pulses. The results are very quick excitations by quantum gates represented by shaped laser pulses such that possibly thousands of gates can be applied before decoherence becomes an issue. Unfortunately, n qubits are represented each by a specific rovibrational state or mode, utilizing 2^n states and posing a problem with scalability. Further suggestions include adopting this method but specifically trapping diatomic molecules in a linear optical trap or optical lattice [36], thus eliminating the issue of scalability. Theoretical research is aimed at providing information regarding laser pulse shaping of the quantum gate, control of the qubit excitations and indication of candidate molecules for such architectures. Experimental investigations are mostly concerned with the preparation of such diatomics and the ability for optical trapping of them.

9.2 Procedure for Performing a Quantum Computation

Quantum computer processing can be broken down into three chronological procedures: (1) system preparation, (2) system manipulation and (3) system readout. Before an algorithm can be implemented, the system must be prepared in the desired initial qubit state arrangement. The qubit states are then manipulated through application of quantum logic gates to carry out the desired algorithm. After the algorithm is complete, the system must be read to determine the solution to the problem. The three general steps are summarized in the following sections. Emphasis is placed on and further details are provided for the system manipulation

step in subsequent sections, since understanding this step theoretically involves the utilization of quantum dynamics techniques.

9.2.1 System Preparation: Qubit Initialization

With respect to implementing a quantum algorithm, the set of n qubits must be initialized. This requires preparing the quantum system into a known configuration or, more specifically, preparing the qubits into a known and desired state. The initial state of the qubits depends on the problem being studied. Generally this is carried out through common atomic or, more recently, molecular [37] "cooling" techniques, where the system is brought ideally to its ground quantum state with respect to the qubit representation. Thus, after cooling, the system is prepared into a state where all qubits have been initialized, for instance a register reading as $|000\ldots0\rangle$, depending on how many qubits are used. If the ground state is not a qubit representation, then further excitations must occur in order to create an initialized qubit register. There are clearly obvious advantages to having the initial qubit representation being that of the ground quantum state.

9.2.2 System Manipulation: Apply Quantum Algorithms

After the qubits have been specifically prepared, the quantum algorithm is then applied via qubit manipulation through the necessary quantum logic gates. Laser pulses, or more generally electromagnetic fields, provide a practical means to implement the quantum logic gates and manipulate the quantum states of atoms and molecules. Such experimental implementations include NMR [6–8] and ion trap quantum computing [17, 38], with applied laser pulses using radiowave and microwave frequencies, respectively. An alternative quantum computer architecture proposed suggests using the rovibrational states of molecules as qubits and producing mid-infrared laser pulses to represent the quantum logic gates [9]. Within the mid-IR frequency region, laser pulses can be generated which are ultrafast (fs to ps duration) and whose time-domain (spectral) properties are well controlled. These properties allow the precise implementation of quantum gates and application of quantum algorithms in time frames before decoherence becomes problematic. Much of the theoretical work within molecular quantum computing has focused on the quantum dynamics involved during the qubit manipulation step. The primary concern is to obtain insight with respect to the laser pulse representation of quantum logic gates, the controllability of the qubits, issues governing decoherence and the sensitivity to the choice of molecular system. The effect of shaping laser pulses to represent quantum logic gates, qubit controllability and the choice of molecular system will be covered in Sect. 9.3, for the proposed quantum computing architecture using the rovibrational states of diatomics (or polyatomics) as qubits and shaped laser pulses as quantum logic gates.

9.2.3 System Readout: Determine the Solution

Once the quantum algorithm has been implemented on the qubits, the solution to the problem must be determined. This amounts to determining (i.e. measuring) the final quantum state of the qubits. Unlike in classical computing, the act of measuring the quantum system destroys the qubit arrangement and so readout can only occur once per calculation. In theory, this is sufficient since we do not need to carry out identical calculations to determine a solution. In practice, measurements are not without error and generally there is an error associated with determining the state of the qubits. Thus far, the simple quantum algorithms that have been carried out to show quantum computation have in general relied on repeat measurements to improve the probability of the solution. In the case of NMR quantum computing, the qubit states are superimposed on an ensemble rather than individual molecules, and thus measuring the nuclear spin qubit state occurs over a statistical average [6]. Readout on ion trap quantum computers has been carried out by exciting to a higher lying electronic state and, by monitoring the fluorescence, the original qubit states can be determined [32]. In classical computer systems, there are also associated errors but their probability has been dramatically decreased through fault tolerance techniques and improved technology. Analogous quantum error correction and fault tolerant techniques [39] as well as new readout methods, see for example [40], to improve quantum computing are being developed, proposed and researched.

9.3 Molecular Quantum Computing Using Shaped Laser Pulses

In an attempt to expand the search for quantum computing architectures, it was suggested that the rovibrational states or modes of molecules could be used as the qubit representation and laser pulses could be shaped to cause the required quantum logic gate operation on the qubits [9]. This came at a time when there were emerging chemistry experiments being performed with mid-infrared shaped laser pulses on the femtosecond time scale, with control of phase and amplitude at specific frequencies [41]. It was thought that the quantum algorithm could be applied more quickly with picosecond laser pulses (mid-infrared) than with pulses used in ion traps (microwave; nanosecond) or NMR (radiowave; microsecond) quantum architectures; thus possibly minimizing decoherence issues. Internal molecular modes and rovibrational transitions are also more strongly coupled, in comparison with ion trap and NMR quantum computing implementations. Numerous theoretical studies emerged examining the use of internal vibrational modes of polyatomics (e.g. acetylene [42, 43], ammonia [44, 45], thiophosgene [18, 46, 47], vibrational [48] or rovibrational states of diatomics [49–51] and also systems using dipole–dipole coupled diatomics [52–55] as the qubits. The majority of theoretical studies determined the optimal shape of the laser pulse using OCT [56, 57], while others implemented optimization routines such as ant colony optimization [58], Simulated

Annealing [59] or, more commonly, Genetic Algorithm (GA) optimization [50, 51, 60]. In this section, we introduce the relevant dynamics equations, how OCT or GA procedures differ and how they are utilized for the required qubit transformations for logic gate representation, including global phase alignment. In general, the theory is presented for diatomic molecules, but the generalization to polyatomics is straightforward, for example, see [45] where MCTDH is utilized to examine gate operations in ammonia.

9.3.1 Quantum Dynamics: Laser/Molecule Interaction

The molecular response to the laser pulse is determined by solving the TDSE,

$$i\hbar \frac{d\Psi(t)}{dt} = \hat{H}\Psi(t). \tag{9.2}$$

The semi-classical Hamiltonian, $\hat{H}$, composed of a time-independent operator $\hat{H}_0$, describing the molecule, combined with the time-dependent term describing the interaction of the electric field, $\epsilon(t)$, with the molecular dipole moment, $\mu(r)$, is given by,

$$\hat{H} = \hat{H}_0 - \boldsymbol{\mu}(r) \cdot \boldsymbol{\epsilon}(t) = \hat{H}_0 - \mu(r)\epsilon(t)\cos\theta. \tag{9.3}$$

The wavefunction, $\Psi(t)$, composed of a linear combination of time-dependent coefficients, $c_{vJ}(t)$, with rovibrational state eigenvectors $|vJ\rangle$ is described by,

$$\Psi(t) = \sum_{vJ} c_{vJ}(t)|vJ\rangle. \tag{9.4}$$

The magnetic quantum number M is equal to zero for the closed shell diatomic molecules and linear electric field polarizations considered in our pulse optimization examples. However, in general, one may have to consider a sum over quantum number M (for open shell systems), other hyperfine constants and/or multiple vibrational states (for polyatomics).

Solving the TDSE for the time-dependent coefficients in vector notation, $\underline{c}(t)$, results in,

$$\dot{\underline{c}}(t) = -\frac{i}{\hbar}\left[\underline{\underline{E}} - \epsilon(t)\underline{\underline{\mu}}\right]\underline{c}(t). \tag{9.5}$$

Each time step along the laser pulse duration can be solved by using a numerical integrator such as the commonly used Runge–Kutta fourth order integrator. Care must be taken to ensure that the time steps are smaller than the oscillatory period of the laser pulse in order to minimize integration error. The diagonal rovibrational state energy matrix, $\underline{\underline{E}}$, is

$$\underline{\underline{E}} = \begin{pmatrix} E_{0,0} & 0 & \cdots & 0 \\ 0 & E_{0,1} & \cdots & 0 \\ \vdots & \vdots & \ddots & \vdots \\ 0 & 0 & \cdots & E_{\nu_{\max},J_{\max}} \end{pmatrix} \tag{9.6}$$

where $\nu_{\max}$ and $J_{\max}$ are the maximum vibrational and rotational states, respectively, considered when solving the problem of interest numerically. The energies can be determined directly from experimental spectroscopic excitation data, from fits of diatomic molecular constants or through numerical calculations of the quantum states from an ab initio potential energy curve. Rather than using a basis of eigenstates, one can solve the problem using the potential energy curve, $V(r)$, or surface (for polyatomics), directly [45]. An example of the transition dipole moment matrix, $\underline{\underline{\mu}}$, is shown for single photon excitations between adjacent rovibrational states,

$$\underline{\underline{\mu}} = \mu_{\nu,J}^{\nu',J'} = \begin{pmatrix} 0 & \mu_{0,J}^{1,J'} & 0 & & 0 & 0 & 0 \\ \mu_{1,J}^{0,J'} & 0 & \mu_{1,J}^{2,J'} & \cdots & & 0 & 0 \\ 0 & \mu_{2,J}^{1,J'} & 0 & & & & 0 \\ & \vdots & & \ddots & & \vdots & \\ 0 & & & & \mu_{\nu_{\max}-2,J}^{\nu_{\max}-1,J'} & 0 & \\ 0 & 0 & & \cdots & \mu_{\nu_{\max}-1,J}^{\nu_{\max}-2,J'} & 0 & \mu_{\nu_{\max}-1,J}^{\nu_{\max},J'} \\ 0 & 0 & 0 & & 0 & \mu_{\nu_{\max},J}^{\nu_{\max}-1,J'} & 0 \end{pmatrix}. \tag{9.7}$$

It is tridiagonal with zeroes along the diagonal and structured so that excitations occur via simultaneous $\Delta\nu = \pm 1$ and $\Delta J = \pm 1$ transitions as is appropriate for a relatively weak, linearly polarized laser field. The notation for $\underline{\underline{\mu}}$ is given by initial state (ν,J) as a subscript and the final state, (ν',J'), as a superscript. Equation (9.7) shows the structure for vibrational transitions and Eq. (9.8) shows the rotational transition substructure of the sample cell at $\mu_{0,J}^{1,J'}$

$$\mu_{0,J}^{1,J'} = \begin{pmatrix} 0 & \mu_{0,0}^{1,1} & 0 & & 0 & 0 & 0 \\ \mu_{1,1}^{0,0} & 0 & \mu_{0,1}^{1,2} & \cdots & & 0 & 0 \\ 0 & \mu_{1,2}^{0,1} & 0 & & & & 0 \\ & \vdots & & \ddots & & \vdots & \\ 0 & & & & \mu_{0,J_{\max}-2}^{1,J_{\max}-1} & 0 & \\ 0 & 0 & & \cdots & \mu_{1,J_{\max}-1}^{0,J_{\max}-2} & 0 & \mu_{0,J_{\max}-1}^{1,J_{\max}} \\ 0 & 0 & 0 & & 0 & \mu_{1,J_{\max}}^{0,J_{\max}-1} & 0 \end{pmatrix}. \tag{9.8}$$

The exact form of the transition dipole matrix will vary depending on the excitations involved. Initial investigations into the state population transfer are

required since the number of quantum states included in the computations involves a truncation of the complete set at $(v_{\max}, J_{\max})$. The total number of states required in the computation is dependent on the quantum states used as the qubits, the strength of the state-to-state coupling and also the strength of the laser pulse being optimized. In general, one is looking to include a minimum number of states such that insignificant population transfer occurs for higher lying quantum states and the resulting sum of the populations of the included states resembles to some error the condition if all quantum states were included.

In relation to quantum computing, Eq. (9.5) illustrates that the resulting time-dependent coefficient corresponding to each qubit at the final time needs to be determined in order to elucidate effectiveness of the laser pulse ($\epsilon(t)$) at representing the quantum logic gate. The two most common theoretical methods used to determine the optimized laser pulse to represent specific quantum logic gates will be discussed in the next sections, namely OCT and GA optimization.

9.3.2 Optimal Control Theory (OCT)

One of the most widely used theoretical laser optimization routines for molecular laser control is OCT due to its relative ease in implementation and monotonic convergence, see recent reviews [12–14] and the many references therein. Optimization of the laser pulse occurs in the time-domain. Beyond the initial implementation [61], further investigations developed important features such as constraints on the frequency spectrum[62–64] and optimization of the laser pulse duration[65–67], both of which are required to produce laser pulses comparable to those obtained experimentally. Within OCT an objective function, J, is maximized according to constraints on the required excitation, constraints on the laser pulse field and it must also satisfy the TDSE. These constraints are represented by each term in the objective function, respectively,

$$J = \sum_{k}^{z} \left| \left\langle \Psi_i^k(T) | \Phi_f^k \right\rangle \right|^2 - \int_0^T \frac{\alpha_0}{s(t)} |\epsilon(t)|^2 \, dt$$
$$-2Re \sum_{k}^{z} \left[\left\langle \Psi_i^k(T) | \Phi_f^k \right\rangle \int_0^T \left\langle \Psi_f^k(t) \left| i \left[H_0 - \mu\epsilon(t) \right] + \frac{\partial}{\partial t} \right| \Psi_i^k(t) \right\rangle dt \right]. \tag{9.9}$$

Here Ψ_i^k is the resulting wavefunction after interaction with the laser pulse (of total pulse duration T) of the ith state for the kth qubit transformation for the specific quantum logic gate. Φ_f^k is the target state of the qubit transformation for the specific quantum logic gate. The second term in the objective function contains the electric field, $\epsilon(t)$, and the penalty parameter, α_0, which is an arbitrary constant that determines the weight of the field term on the resulting objective function, J.

The penalty parameter is important for appropriate laser pulse optimization and chosen based upon numerical adjustments. The integer z corresponds to the number of multiple target qubit states that are being optimized to represent the quantum logic gate. For 1-qubit operations, $z = 2$ and for 2-qubit operations, $z = 4$.
Upon maximizing the objective function with respect to $\Psi_i^k(t)$, $\Psi_f^k(t)$ and $\epsilon(t)$, a set of resultant equations is obtained [68]:

$$i\frac{\partial}{\partial t}\Psi_i^k(t) = [H_0 - \mu\epsilon(t)]\,\Psi_i^k(t), \qquad \Psi_i^k(0) = \Phi_i^k, \quad k = 1\ldots z \tag{9.10}$$

$$i\frac{\partial}{\partial t}\Psi_f^k(t) = [H_0 - \mu\epsilon(t)]\,\Psi_f^k(t), \qquad \Psi_f^k(0) = \Phi_f^k, \quad k = 1\ldots z \tag{9.11}$$

$$\epsilon(t) = -\frac{zs(t)}{\alpha_0}\sum_k^z Im\left\{\left\langle\Psi_i^k(t)|\Psi_f^k(t)\right\rangle \times \left\langle\Psi_f^k(t)|\mu|\Psi_i^k(t)\right\rangle\right\}. \tag{9.12}$$

The first two conditions are the TDSE describing the wavefunctions $\Psi_i^k(t)$ and $\Psi_f^k(t)$, while the last equation details the form of the laser pulse, $\epsilon(t)$. There are several numerical methods that have been developed to solve for the laser pulse field using the above optimal equations, see [14]. It is important to note that the optimal pulses obtained by alternative methods for numerical optimization can differ [69] and this is a reflection that there are generally numerous pathways/solutions to the required problem.

The laser pulse envelope, $s(t)$ with amplitude s_0, is arbitrary but is usually defined by a *sine-squared* envelope or *Gaussian* envelope with pulse width σ, respectively:

$$s(t) = s_0 \sin^2(\pi t/T) \tag{9.13}$$

$$s(t) = s_0 \exp\left(-\frac{(t-\frac{T}{2})^2}{2\sigma^2}\right). \tag{9.14}$$

As stated previously, the quantum gate operation being represented by the optimized laser pulse not only induces a change in population but must also induce a global phase alignment between the qubits (see Sect. 9.1.1). We shall see that in the GA this is accomplished through an appropriately chosen fidelity function, F (Eq. (9.22)). The simplest process of including global phase alignment within OCT though, without altering the objective function and thus subsequent maximization, is to include an auxiliary transition into the optimization [68]:

$$[|\Psi_{00}\rangle + |\Psi_{01}\rangle + |\Psi_{10}\rangle + |\Psi_{11}\rangle]_{t=0} \longrightarrow \left[(|\Psi_{00}\rangle + |\Psi_{01}\rangle + |\Psi_{10}\rangle + |\Psi_{11}\rangle)e^{i\phi_5}\right]_{t=T} \tag{9.15}$$

This fifth stipulation on the requirement for the resultant optimized laser field is incorporated within the summation of the first term of the objective function

(Eq. (9.9)), now with $z = 5$ for 2-qubit operations. The qubits, after operation by the laser pulse, are then biased to shift by the same amount of phase, $e^{i\phi}$ (global phase alignment). Phase alignment is in general more difficult to optimize than population.

9.3.3 Genetic Algorithm (GA) Optimization

The Genetic Algorithm is a heuristic search optimization routine that utilizes ideas from natural selection to "breed" laser pulses, in effect optimizing the associated pulse parameters (e.g. phase and amplitude), to produce the "fittest" or optimal pulse shape [70]. In comparison with OCT, the GA optimizes the laser pulse in the frequency domain with associated pulse parameters and is constructed in the time-domain through a Fourier transform. Since OCT is monotonically convergent then a convergence criteria can be readily implemented indicating progress in locating the optimal pulse chape. Conversely, in GA optimizations since the parameter space is being searched, there is no guideline dictating how many more generations will be needed to bring the fidelity up to a specific value indicative of the optimal pulse. On the other hand, without specific OCT pulse constraints, the optimal laser pulses generated do not necessarily represent those obtainable from current experimental laser pulse shaping techniques, see, however, recent work by Shyslov and Babikov [46]. Work has been done using variations to both the GA and OCT optimizations in order to bridge the gap between optimal pulses obtained from theory and those obtained from experiment [71].

In Fig. 9.1, the general framework of a closed-loop feedback set-up using a GA is conceptualized. Initially a random set of laser pulses, experimental or theoretical, is input into the quantum dynamics procedure (Fig. 9.1; lower box) in order to start the algorithm. The upper box is the GA routine, constituting the laser pulse optimization. In the theoretical case, the quantum dynamics is determined by solving the TDSE for the applied laser pulse, from an initial state Ψ_i, over the laser pulse duration, to a final state Ψ_f. The Fidelity (see Sect. 9.3.3.2), a value between 0 and 1, is computed which describes the effectiveness of the specific laser pulse at carrying out the required quantum gate operation over the chosen rovibrational state qubits. This is repeated for all laser pulses of that generation. The Fidelity is fed back into the GA so that it can rank the laser pulses and determine the appropriate actions for "breeding". A new set of laser pulses is produced which constitutes the next generation. This process is continued for n generations. Both the GA and quantum dynamics are connected in a closed loop, providing feedback to each other in order to produce an optimal pulse for the quantum gate operation of interest.

9.3.3.1 Laser Field

In general, a laser field (electromagnetic radiation) is modelled classically as a combination of perpendicular oscillating electric and magnetic fields. The electric field interaction with the electric dipole moment is (typically) five orders-of-magnitude (10^5 times) larger than the magnetic field interaction with the magnetic dipole [72]. Therefore, effects of the magnetic dipole are omitted in theoretical investigations

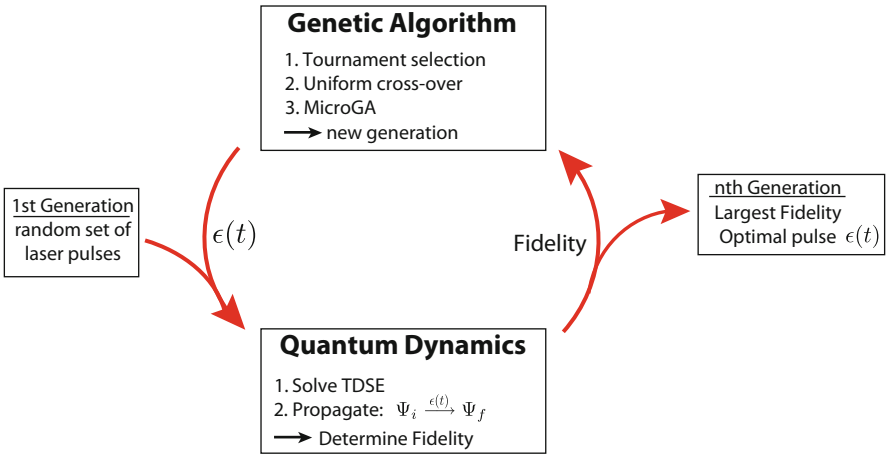

Fig. 9.1 Illustration of theoretical shaped laser pulse optimization using a genetic algorithm (GA). The first generation of laser pulses is randomly generated. The time-dependent Schrödinger equation (TDSE) for the model diatomic is solved for each input laser pulse. The system is propagated from an initial state Ψ_i to a final state Ψ_f, at which point the fidelity is calculated based upon how close the laser pulse brings the system to the desired final state. The fidelity associated with each laser pulse is used to determine the GA optimization through tournament selection and uniform cross-over. The GA produces a new generation of laser pulses related to the previous ones. The cycle is repeated for n generations; the optimal laser pulse being produced in the nth generation

and only the electric field/electric dipole moment interaction is considered. In molecular quantum computing applications, the effect of polarizability has also been considered [49] but its effects were shown to be negligible for the fields considered—fields which are typical of most theoretical simulations in this area.

As stated by Milonni [73], "An arbitrarily large number n of 'photons' may occupy the same state, and when this situation obtains, it is accurate to regard the photon wave function as defining a classical field distribution." Thus the quantum electrodynamic view of radiation for intense laser fields can be described classically. Overall, the light–matter interaction is treated semi-classically where the diatomic molecule is quantum mechanical and the laser pulse is classical in nature. The electric dipole approximation [74] is also used which reduces the form of the electric field due to the comparative size of the electric field wavelength compared to the molecule. The classical description of the laser field, $E(r,t)$, can be written in complex form according to

$$E(r,t) = \epsilon_0 \cos(\omega t - \mathbf{k}\cdot\mathbf{r}) = \epsilon_0 \Re\left[e^{i\omega t} e^{-i\mathbf{k}\cdot\mathbf{r}}\right]. \tag{9.16}$$

It is a continuous laser field of single-frequency (ω) with peak field strength (ϵ_0) being a function of space and time. The norm of the wave vector ($\mathbf{k}$) is related to the frequency of the laser field by $k = \frac{\omega}{c}$, and for example is on the order of 10^{-6} Å^{-1}

for the mid-infrared frequencies. The value of k describes the number of oscillations of the electric field in space. In this case one oscillation occurs approximately every 10^6 Å, which is much larger than the molecules studied in molecular quantum computing. Consequently the resulting value of $\mathbf{k} \cdot \mathbf{r}$ is small and the Taylor series expansion for the electric field of the laser can be truncated to the first term (i.e., unity):

$$e^{-ik\mathbf{n}\cdot\mathbf{r}} = 1 - [i\,\mathbf{k}\cdot\mathbf{r}] + \frac{1}{2}[-i\,\mathbf{k}\cdot\mathbf{r}]^2 + \cdots \approx 1. \tag{9.17}$$

The electric field can now be written strictly in terms of time,

$$E(r,t) = \epsilon_0 \Re\left[e^{i\omega t}\right] = \epsilon_0 \cos(2\pi\nu t). \tag{9.18}$$

For the example optimized laser pulses illustrated herein, only the amplitude and phase were shaped (no polarization shaping [75, 76] was considered). The pulse shaping occurs in the frequency domain which can be readily connected to the more familiar time-domain expression for the laser field. The form of the laser pulse for each component of the discretized frequency spectrum with amplitude and phase variation is [49]

$$\epsilon(\nu_j) = \epsilon_0 \sqrt{A(\nu_j)} \exp\left[-2\ln 2\left(\frac{\nu_j - \nu_0}{\Delta\nu}\right)^2\right] \exp\left[i\phi(\nu_j)\right]. \tag{9.19}$$

In Eq. (9.19), ϵ_0 is the peak field strength, ν_0 is the central frequency and ν_j represents the discrete frequencies at which the field is shaped. A Gaussian envelope is used with a full width at half-maximum (FWHM) pulse width of $\Delta\nu$. The amplitude and phase range from $0 \le A(\nu_j) \le 1$ and $0 \le \phi(\nu_j) \le 2\pi$, respectively. A transformed-limited (TL) pulse corresponds to the case when $A(\nu_j) = 1$ and $\phi(\nu_j) = 0$ for all frequency components j. The familiar time-dependent form of the laser pulse can be determined by a Fourier transform or alternatively using the analytic form for the time-dependent field [77]:

$$\epsilon(t) = \frac{\sin(\pi t d\nu)}{\pi t} \sum_{j=0}^{n} \epsilon_0 \sqrt{A_j} \exp\left[-2\ln 2\left(\frac{\nu_j - \nu_0}{\Delta\nu}\right)^2\right] \cos(2\pi\nu_j t + \phi_j), \tag{9.20}$$

with frequency resolution $d\nu$. The frequency domain laser pulse shaping shown is closely related to experimental Spatial Light Modulators using Liquid Crystal pixelated grids (LC-SLM). This requires diffraction of the incident laser pulse onto the LC-SLM, in which each pixel will be illuminated by a specific frequency band. At each pixel, there is simultaneous control over the amount of light transmitted (amplitude) and the phase of that light passing through. Once each frequency band passes through and is affected by the LC-SLM, the light is recombined to form a

new pulse shape depending on the alterations imposed by the shaper. Thus, there are numerous pulse shapes that can be generated by varying for instance: the number of frequency bands (ν_j), the resolution of the frequency bands illuminating each pixel ($d\nu$) and the variation in amplitude and phase. The GA optimization aims at modelling an LC-SLM set-up in order to reflect more closely the possible laser pulse shapes that can be experimentally produced.

9.3.3.2 Fidelity and Average Population

Within GA optimization, the degree to which the shaped laser pulse represents the quantum logic gate operation of interest is stated by a metric. Initial theoretical studies which had not yet perceived the necessity of global phase alignment used the average population $\bar{P}$, as this metric, i.e.,

$$\bar{P} = \frac{1}{N} \sum_{k=1}^{N} |\langle \Psi_k(T) | \Phi_k \rangle|^2 , \tag{9.21}$$

where $\Psi_k(T)$ is the resulting wavefunction after the laser pulse of duration T has been applied and Φ_k is the target wavefunction. The sum is over the number of qubit transformations N, which is $N = 4$ for the case of 2-qubit operations. There is clearly no phase information contained in the average population function. Population transfer combined with global phase alignment can be included in the required constraints for shaped laser pulses within the GA by using instead the fidelity function, F, where

$$F = \frac{1}{N^2} \left| \sum_{k=1}^{N} \langle \Psi_k(T) | \Phi_k \rangle \right|^2 . \tag{9.22}$$

The fidelity is a number between 0 and 1. $F = 0$ implies no excitation to the resultant qubit state (i.e., an incomplete quantum gate operation), while $F = 1$ implies a 100 % complete quantum gate operation on the qubits. Though the average population is a useful value to determine the extent of overall population transfer between the qubits, it is strictly the fidelity function values that should be used within the GA optimization procedure when dealing with quantum gate operations.

9.4 Summary and Future Directions

In the present work, the basic ideas of quantum computing have been presented by highlighting the similarities and differences to classical computing, see Sects. 9.1.1 and 9.1.2. Most important among these differences is the possibility for exponential speed-up in solving computational problems, if, and only if, suitable quantum algorithms can be designed, see Sects. 9.1.3 and 9.1.4. In addition to the development of quantum algorithms, a critical choice is the physical system on which the quantum gates, and hence algorithms, can be implemented, see Sect. 9.1.6, where

the primary focus is on atomic and molecular systems. Once a physical system has been chosen (in this work, the discussion is on molecules), there are three important steps: (i) system preparation, (ii) gate and algorithm implementation and (iii) system readout, see Sects. 9.2.1–9.2.3. The majority of the research on molecular quantum computing has emphasized step (ii), see for example [18,42–55]. Therefore, the theoretical investigation of molecular quantum computing involves several important elements: the choice of molecular (hyperfine, rovibrational, rovibronic. . .) states for the qubits and the molecule from which they are selected, the quantum gates to be implemented, and the optimization algorithm used to determine the laser field. The two most important computational challenges presented for gate implementation, i.e., step (ii), are the accurate and efficient solution of the TDSE, see Sect. 9.3.1, and the optimization techniques used to find the required laser field, see Sects. 9.3.2 and 9.3.3. Unlike control of photochemical or photo physical processes, molecular quantum computing imposes the stringent requirement of global phase alignment for quantum gate operations. While initial studies of molecular quantum computing have been promising, practical applications involving several (or many) qubits remain challenging. These will require the careful choice of a molecular system for scalability, e.g., the use of coupled polar diatomic molecules on a 1D array[36, 37, 53–55]. However, just as important will be the development of new or refined theoretical and computational techniques for dealing with quantum dynamics (most likely, for many degrees of freedom) and/or optimization algorithms for finding the best (and, hopefully, experimentally accessible) laser field. Whatever approach is taken, insight can, and will, be revealed through high-level simulations.

Acknowledgements The authors thank the Alberta Ingenuity Fund (New Faculty Award) and the Natural Sciences and Engineering Research Council of Canada (NSERC Discovery Grant) for financial support. We thank the Canadian Foundation for Innovation (New Opportunities Fund) for support of the computational infrastructure on which this work was carried out. R.R.Z. acknowledges financial support of NSERC via a PGS-D2 scholarship.

References

1. Feynman R (1982) Simulating physics with computers. Int J Theor Phys 21:467
2. Nielsen MA, Chuang IL (2000) Quantum computation and quantum information. Cambridge University Press, Cambridge
3. Benenti G, Casati G, Strini G (2004) Principles of quantum computation and information, vol I: basic concepts. World Scientific, Singapore
4. Cirac JI, Zoller P (1995) Quantum computations with cold trapped ions. Phys Rev Lett 74:4091
5. Chotia A, Neyenhuis B, Moses S, Yan B, Covey J, Foss-Feig M, Rey AM, Jin DS, Ye J (2012) Long-lived dipolar molecules and Feshbach molecules in a 3D optical lattice. Phys Rev Lett 108:080405
6. Vandersypen LMK, Steffen M, Breyta G, Yannoni CS, Sherwood MH, Chuang IL (2001) Experimental realization of Shor's quantum factoring algorithm using nuclear magnetic resonance. Nature 414:883
7. Chuang IL, Vandersypen LMK, Zhou XL, Leung DW, Lloyd S (1998) Experimental realization of a quantum algorithm. Nature 393:143

8. Jones JA, Mosca M (1998) Implementation of a quantum algorithm on a nuclear magnetic resonance quantum computer. J Chem Phys 109:1648
9. Tesch CM, de Vivie-Riedle R (2002) Quantum computation with vibrationally excited molecules. Phys Rev Lett 89:157901
10. Zadoyan R, Kohen D, Lidar DA, Apkarian VA (2001) The manipulation of massive ro-vibronic superpositions using time-frequency-resolved coherent anti-stokes Raman scattering (TFR-CARS): from quantum control to quantum computing. Chem Phys 266:323
11. Bihary Z, Glenn DR, Lidar DA, Apkarian VA (2002) An implementation of the Deutsch-Jozsa algorithm on molecular vibronic coherences through four-wave mixing: a theoretical study. Chem Phys Lett 360:459
12. Brif C, Chakrabarti R, Rabitz H (2010) Control of quantum phenomena: past, present and future. New J Phys 12:075008
13. Brif C, Chakrabarti R, Rabitz H (2012) Control of quantum phenomena. Adv Chem Phys 148:1
14. Balint-Kurti GG, Zou S, Brown A (2008) Optimal control theory for manipulating molecular processes. Adv Chem Phys 138:43
15. Knill E, Laflamme R, Martinez R, Tseng CH (2000) An algorithmic benchmark for quantum information processing. Nature 404:368
16. Schmidt-Kaler F, Häffner H, Riebe M, Gulde S, Lancaster GPT, Deuschle T, Becher C, Roos CF, Eschner J, Blatt R (2003) Realization of the Cirac–Zoller controlled-NOT quantum gate. Nature 422:408
17. Gulde S, Riebe M, Lancaster GPT, Becher C, Eschner J, Haffner H, Schmidt-Kaler F, Chuang IL, Blatt R (2003) Implementation of the Deutsch-Jozsa algorithm on an ion-trap quantum computer. Nature 421:48
18. Weidinger D, Gruebele M (2007) Quantum computation with vibrationally excited polyatomic molecules: effects of rotation, level structure, and field gradients. Mol Phys 105:1999
19. Vala J, Amitay Z, Zhang B, Leone SR, Kosloff R (2002) Experimental implementation of the Deutsch-Jozsa algorithm for three-qubit functions using pure coherent molecular superpositions. Phys Rev A 66:062316
20. Ahn J, Bucksbaum PH, Weinacht TC (2000) Information storage and retrieval through quantum phase. Science 287:463
21. Bomble L, Lauvergnat D, Remacle F, Desouter-Lecomte M (2008) Vibrational computing: simulation of a full adder by optimal control. J Chem Phys 128:064110
22. Deutsch D (1985) Quantum theory, the Church-Turing principle and the universal quantum computer. Proc R Soc Lond Ser A 400:97
23. Shor PW (1997) Polynomial-time algorithms for prime factorization and discrete logarithms on a quantum computer. SIAM J Comput 26:1484
24. Aspuru-Guzik A, Dutoi AD, Love PJ, Head-Gordon M (2005) Simulated quantum computation of molecular energies. Science 309:1704
25. Kassal I, Jordan SP, Love PJ, Mohseni M, Aspuru-Guzik A (2008) Polynomial-time quantum algorithm for the simulation of chemical dynamics. Proc Natl Acad Sci 105:18681
26. Wang H, Ashhab S, Nori F (2011) Quantum algorithm for simulating the dynamics of an open quantum system. Phys Rev A 83:062317
27. Kassal I, Aspuru-Guzik A (2009) Quantum algorithm for molecular properties and geometry optimization. J Chem Phys 131:224102
28. Yung MH, Aspuru-Guzik A (2012) A quantum quantum Metropolis algorithm. Proc Natl Acad Sci 109:754
29. Destainville N, Georgeot B, Giraud O (2010) Quantum algorithm for exact Monte Carlo sampling. Phys Rev Lett 104:250502
30. Harrow AW, Hassidim A, Lloyd S (2009) Quantum algorithm for linear systems of equations. Phys Rev Lett 103:150502
31. Cao Y, Papageorgiou A, Petras I, Traub J, Kais S (2013) Quantum algorithm and circuit design solving the Poisson equation. New J Phys 15:013021
32. Monz T, Schindler P, Barreiro JT, Chwalla M, Nigg D, Coish WA, Harlander M, Hänsel W, Hennrich M, Blatt R (2011) 14-Qubit entanglement: creation and coherence. Phys Rev Lett 106:130506

33. DiVincenzo DP, Loss D (1998) Quantum information is physical. Superlattice Microstruct 23:419
34. Kielpinski D, Monroe C, Wineland DJ (2002) Architecture for a large-scale ion-trap quantum computer. Nature 417:709
35. Lanyon BP, Whitfield JD, Gillett GG, Goggin ME, Almeida MP, Kassal I, Biamonte JD, Mohseni M, Powell BJ, Barbieri M, Aspuru-Guzik A, White AG (2010) Towards quantum chemistry on a quantum computer. Nat Chem 2:106
36. DeMille D (2002) Quantum computation with trapped polar molecules. Phys Rev Lett 88:067901
37. Carr LD, Demille D, Krems RV, Ye J (2009) Cold and ultracold molecules: science, technology and applications. New J Phys 11:055049
38. Sackett CA, Kielpinski D, King BE, Langer C, Meyer V, Myatt CJ, Rowe M, Turchette QA, Itano WM, Wineland DJ, Monroe C (2000) Experimental entanglement of four particles. Nature 404:256
39. Devitt SJ, Munro WJ, Naemoto K (2013) Quantum error correction for beginners. Rep Prog Phys 76:076001
40. Vincent R, Klyatskaya S, Ruben M, Wernsdorfer W, Balestro F (2012) Electronic readout of a single nuclear spin using a molecular spin transistor. Nature 488:357
41. Nuernberger P, Vogt G, Brixner T, Gerber G (2007) Femtosecond quantum control of molecular dynamics in the condensed phase. Phys Chem Chem Phys 9:2470
42. Tesch CM, Kurtz L, de Vivie-Riedle R (2001) Applying optimal control theory for elements of quantum computation in molecular systems. Chem Phys Lett 343:633
43. Troppmann U, Tesch CM, de Vivie-Riedle R (2003) Preparation and addressability of molecular vibrational qubits in the presence of anharmonic resonance. Chem Phys Lett 378:273
44. Suzuki S, Mishima K, Yamashita K (2005) Ab initio study of optimal control of ammonia molecular vibrational wavepackets: towards molecular quantum computing. Chem Phys Lett 410:358
45. Schroeder M, Brown A (2009) Realization of the CNOT quantum gate operation in 6D ammonia using the OCT-MCTDH approach. J Chem Phys 131:034101
46. Shyshlov D, Babikov D (2012) Complexity and simplicity of optimal control theory pulses shaped for controlling vibrational qubits. J Chem Phys 137:194318
47. Berrios E, Gruebele M, Shyshlov D, Wang L, Babikov D (2012) High fidelity quantum gates with vibrational qubits. J Phys Chem A 116:11347
48. Babikov D (2004) Accuracy of gates in a quantum computer based on vibrational eigenstates. J Chem Phys 121:7577
49. Tsubouchi M, Momose T (2008) Rovibrational wave-packet manipulation using shaped midinfrared femtosecond pulses toward quantum computation: optimization of pulse shape by a genetic algorithm. Phys Rev A 77:052326
50. Zaari RR, Brown A (2011) Effect of diatomic molecular properties on binary laser pulse optimizations of quantum gate operations. J Chem Phys 135:044317
51. Zaari RR, Brown A (2010) Quantum gate operations using midinfrared binary shaped pulses on the rovibrational states of carbon monoxide. J Chem Phys 132:014307
52. Mishima K, Yamashita K (2009) Quantum computing using rotational modes of two polar molecules. Chem Phys 361:106
53. Jaouadi A, Barrez E, Justum Y, Desouter-Lecomte M (2013) Quantum gates in hyperfine levels of ultracold alkali dimers by revisiting constrained-phase optimal control design. J Chem Phys 139:014310
54. Pellegrini P, Vranckx S, Desouter-Lecomte M (2011) Implementing quantum algorithms in hyperfine levels of ultracold polar molecules by optimal control. Phys Chem Chem Phys 13:18864
55. Bomble L, Pellegrini P, Ghesquière P, Desouter-Lecomte M (2010) Toward scalable information processing with ultracold polar molecules in an electric field: a numerical investigation. Phys Rev A 82:062323

56. Peirce AP, Dahleh MA, Rabitz H (1988) Optimal control of quantum-mechanical systems: existence, numerical approximation, and applications. Phys Rev A 37:4950
57. Zhu WS, Botina J, Rabitz H (1998) Rapidly convergent iteration methods for quantum optimal control of population. J Chem Phys 108:1953
58. Gollub C, de Vivie-Riedle R (2009) Modified ant-colony-optimization algorithm as an alternative to genetic algorithms. Phys Rev A 79:021401
59. Guha S, Mukherjee N, Chaudhury P (2012) A simulated annealing based study to design optimum pulses for selective target excitation in vibrational levels. Indian J Phys 86:245
60. Gollub C, de Vivie-Riedle R (2009) Multi-objective genetic algorithm optimization of 2d- and 3d-pareto fronts for vibrational quantum processes. New J Phys 11:013019
61. Zhu WS, Rabitz H (1998) A rapid monotonically convergent iteration algorithm for quantum optimal control over the expectation value of a positive definite operator. J Chem Phys 109:385
62. Gollub C, Kowalewski M, de Vivie-Riedle R (2008) Monotonic convergent optimal control theory with strict limitations on the spectrum of optimized laser fields. Phys Rev Lett 101:073002
63. Schroeder M, Brown A (2009) Generalized filtering of fields in optimal control theory: application to symmetry filtering for quantum gate operations. New J Phys 11:105031
64. Cheng T, Brown A (2006) Pulse shaping for optimal control of molecular processes. J Chem Phys 124:144109
65. Mishima K, Yamashita K (2011) Free-time and fixed end-point multi-target optimal control theory: application to quantum computing. Chem Phys 379:13
66. Mishima K, Yamashita K (2009) Free-time and fixed end-point optimal control theory in quantum mechanics: application to entanglement generation. J Chem Phys 130:034108
67. Tibbetts KWM, Brif C, Grace MD, Donovan A, Hocker DL, Ho TS, Wu RB, Rabitz H (2012) Exploring the tradeoff between fidelity and time optimal control of quantum unitary transformations. Phys Rev A 86:062309
68. Tesch CM, de Vivie-Riedle R (2004) Vibrational molecular quantum computing: basis set independence and theoretical realization of the Deutsch-Josza algorithm. J Chem Phys 121:12158
69. Sola IR, Santamaria J, Tannor DJ (1998) Optimal control of multiphoton excitation: a black box or a flexible toolkit? J Phys Chem A 102:4301
70. Carroll DL (2004) Genetic Algorithm driver v1.7.0. http://www.cuaerospace.com/carroll/ga.html
71. van der Hoff P, Thallmair S, Kowalewski M, Siemering R, de Vivie-Riedle R (2012) Optimal control theory - closing the gap between theory and experiment. Phys Chem Chem Phys 14:14460
72. Brown JM, Carrington A (2003) Rotational spectroscopy of diatomic molecules. Cambridge University Press, Cambridge
73. Milonni PW (1976) Semiclassical and quantum-electrodynamical approaches in nonrelativistic radiation theory. Phys Rep 25:1
74. Bethe HA, Salpeter EE (1957) Quantum mechanics of one- and two-electron atoms. Springer, Berlin
75. Brixner T, Krampert G, Pfeifer T, Selle R, Gerber G, Wollenhaupt M, Graefe O, Horn C, Liese D, Baumert T (2004) Quantum control by ultrafast polarization shaping. Phys Rev Lett 92:208301
76. Brixner T, Gerber G (2001) Femtosecond polarization pulse shaping. Opt Lett 26:557
77. Zaari RR, Brown A (2012) Effect of laser pulse shaping parameters on the fidelity of quantum logic gates. J Chem Phys 137:104306